Quantitative Analysis of Diubiquitin Isomers Using Ion Mobility-Mass Spectrometry

Elizaveta I. Shestoperova[1], Daniil G. Ivanov[1], Eric R. Strieter[1,2]†

[1]Department of Chemistry, University of Massachusetts Amherst, Amherst, Massachusetts, USA

[2]Molecular & Cellular Biology Graduate Program, University of Massachusetts Amherst, Amherst, Massachusetts, USA

†Corresponding Author: Eric R. Strieter (estrieter@umass.edu)

ABSTRACT

The diversity of ubiquitin modifications calls for methods to better characterize ubiquitin chain linkage, length, and morphology. Here, we use multiple linear regression analysis coupled with ion mobility mass spectrometry (IM-MS) to quantify the relative abundance of different ubiquitin dimer isomers. We demonstrate the utility and robustness of this approach by quantifying the relative abundance of different ubiquitin dimers in complex mixtures and comparing the results to the standard, bottom-up ubiquitin AQUA method. Our results provide a foundation for using multiple linear regression analysis and IM-MS to characterize more complex ubiquitin chain architectures.

INTRODUCTION

Protein ubiquitylation plays a pivotal role in most cellular pathways.[1–5] The small protein ubiquitin (Ub) is covalently attached to other proteins through a series of enzymatic steps.[6,7] Once a single Ub is anchored to target protein, subsequent rounds of conjugation can result in the formation of Ub chains. During chain extension, there are seven ε-amino groups (K6, K11, K27, K29, K33, K48, K63) along with an N-terminus (M1) that can be conjugated to the C-terminus of another Ub molecule.[8] The diversity of Ub chains that manifests is astounding.[9] The linkage, length, and degree of chain branching (i.e., how many Ub subunits are modified at more than one site with other Ub molecules) are all variables and each one can control the cellular destiny of the modified protein.[10–12] Characterizing the types of chains attached to a protein-of-interest (POI) is thus critical to understanding how Ub regulates function, stability, and cellular localization.[13]

Mass spectrometry (MS) is the gold standard for characterizing Ub conjugates. Bottom-up approaches are the most common, as proteolytic digestion breaks down Ub conjugates into peptide fragments, which are then analyzed by MS.[14–16] Ubiquitylation sites are identified by a Ub remnant—a diGly motif—attached to the ε-amino group of a lysine or the α-amino group of an N-terminal residue.[17–19] When combined with isotopically labeled peptide standards (i.e., AQUA peptides), this bottom-up approach enables quantitation of the absolute abundance of various Ub chain linkages.[20–22] What bottom-up fails to provide is information on chain length and the extent of branching.[23] These shortcomings have been addressed using top-down and middle-down MS approaches; however, quantitative information on linkage types is lost.[16,24–27]

By separating ions based on size and shape, ion mobility coupled with mass spectrometry (IM-MS) has the potential to inform on all aspects of Ub chains. IM is a measure of the time it takes an ion to drift through a buffer gas, with compact ions of similar charge traveling faster than those that are more elongated due to fewer interactions with the gas.[28,29] Since Ub chains adopt different conformations depending on linkage, length, and degree of branching, IM-MS can, in principle, be used to separate and detect Ub chains of many different topologies present as heterogeneous mixtures.[30–32] In line with this supposition, it was shown that several di-Ub isomers can be distinguished using drift tube IMS (DTIMS),[33] and four di-Ub isomers can be distinguished using T-wave IM-MS by exploiting differences in the degree of unfolding as a function of linkage type.[34] To further advance the use of IM-MS in Ub chain analysis, it is necessary to develop methods that enable relative quantitation of chain linkages in heterogeneous samples.

Here, we describe a mathematical approach to quantifying mixtures of Ub dimers using IM-MS. Calculating the molar fraction of individual chain linkage types in complex mixtures is challenging because the response to changes in fractional composition is non-linear. Using a multiple linear regression analysis approach, we are able to overcome these issues, and mixtures comprising at least four different isomers can be quantified. To assess the utility of our approach we measured the relative abundance of linkages produced during in vitro Ub chain assembly reactions and compared the results to those obtained by bottom-up AQUA analysis. We found

that the molar fraction measured by IM-MS is consistent with AQUA data. Our study thus establishes a foundation for quantifying the relative abundance of different Ub chain linkage types using IM-MS and multiple linear regression analysis.

EXPERIMENTAL METHODS

Generation of ubiquitin chains. K48-linked ubiquitin dimer: 1 mM Ub, 0.3 uM E1, and 2uM Cdc34 were mixed in reaction buffer A (20mM ATP, 10mM $MgCl_2$, 40mM Tris-HCl pH 7.5, 50 mM NaCl, and 1.5 mM DTT) and incubated overnight at 37°C. K63-linked ubiquitin dimer: 0.5 mM Ub, 1.5 uM E1, and 0.75 uM Ubc13-Mms2 were mixed in reaction buffer A and incubated at 37 for 9 h. K6-linked ubiquitin dimer: 2 mM Ub, 1.5 uM E1, 10 uM UbcH7, and 1uM NleL were mixed in reaction buffer A. 5 uM OTUB1 and 3 uM AMSH were added after 3 h of incubation and the mixture was left overnight at 37°C. All synthesized ubiquitin dimers were further purified from the reaction mixture using size exclusion chromatography (Superdex 75) using buffer B (50 mM Tris-HCl pH 7.5, 300 mM NaCl). The M1-linked ubiquitin dimer construct was expressed in Rosetta 2(DE3)pLysS E.coli cells and further purified using strong cation exchange chromatography (buffer C: 50 mM NH_4OAc 1mM EDTA, buffer D: 50 mM NH_4OAc, 1 mM EDTA, 1 M NaCl). The generated ubiquitin dimers were buffer exchanged into MiliQ water. K11-, K29- and K33-linked ubiquitin dimers were purchased from R&D systems Inc. (Minneapolis, MN). Concentrations of all ubiquitin dimers were measured by BCA assay.

ESI-IM-MS analysis. All experiments were performed on Waters Synapt G2 HDMS mass spectrometer in denaturing conditions using NanoLockSpray ion source for offline nanoESI. Each ubiquitin dimer was diluted to a final concentration of 10 uM in 49/50/1% (v/v %) water/methanol/formic acid. Applied instrument conditions: capillary voltage – 1.0 kV, source temperature – 20°C, sampling cone – 30 V, extraction cone – 1.8 V, trap gas flow – 3 mL/min, helium cell gas flow – 180 mL/min, IMS gas flow – 80 mL/min. TWIMS parameters were adjusted to receive the most efficient separation between ubiquitin dimers at highest available wave height – 40 V. CCS calibration was performed by adding 5 uM apo-myoglobin (Sigma-Aldrich, CAS Number 9008-45-1) as an internal standard.
The complex mixtures, containing two to four di-Ub isomers, were obtained by mixing defined amounts of single isomers at the specified molar ratios.

Data analysis. The initial processing of IM data was performed using MassLynx MS Software (Waters Corporation, USA). Extraction of IM spectra was achieved using TWIM extract, and CCS calibration was performed using homemade-written Python scripts.[35] Further data analyses, including construction of calibration curves and deconvolution of complex spectra, were performed using the Software package OriginPro 2021b (OriginLab Corporation, USA).

AQUA quantitation. The enzymatic reaction with 2 mM Ub, 1.5 uM E1, 10 uM UbcH7, and 1 uM NleL was analyzed using AQUA. In-gel digestion of the di-Ub band was performed using TrypsinGold according to the standard AQUA protocol.[21] Orbitrap Fusion and Easy-nLC 1000 (Thermo Inc., San Jose, CA) operating in FT full scan MS mode in the 300-1500 Th range was used for LC-MS analysis. Linear response curves were constructed for K-ε-GG tryptic AQUA peptides (cell signaling technologies). Self-packed UHPLC RP column was run with water:acetonitrile mixtures in the presence of 0.1% formic acid using the following gradient: : 0-10% B 5 min, 10-30% B 40 min, 30-50% B 15 min, 50-95% 3 min, 95% hold 7 min. XIC chromatograms were extracted using QualBrowser (Thermo Inc., San Jose, CA) and then exported to OriginPro for calculation of peak areas.

RESULTS AND DISCUSSION

IM spectra of seven ubiquitin dimers. Previous studies have shown that even under denaturing conditions, the isomers of di-Ub can still be distinguished by IM-MS.[33] We employed similar conditions to resolve the different isomers. As shown in **Figure 1**, all seven di-Ub isomers display distinct IM spectra at different charge states. For instance, the K48-, K63-, and K6-linked dimers have significantly different IM spectra at the +18 charge state, and K11-, M1-, and K48-linked di-Ub are distinguishable at the +21 charge state.

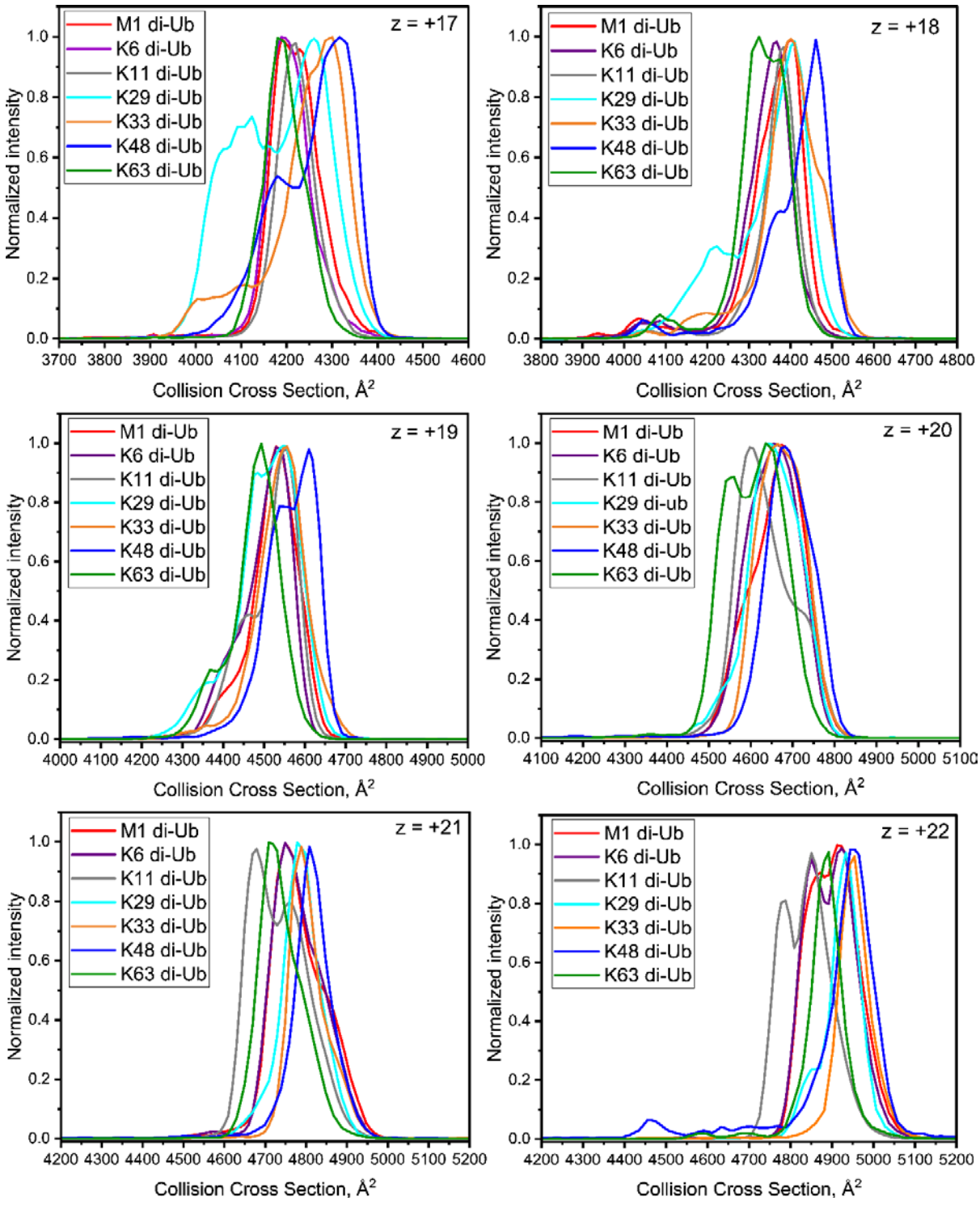

Figure 1. Ion mobility spectra of seven di-Ub isomers under denaturing conditions (49% water, 50% methanol, 1% formic acid) at different charge states: from z = +17 to z = +22.

Use of apo-myoglobin as an internal standard. Quantitative IM-MS is challenging due to the dependence of IM distribution on external conditions and the ESI MS experimental setup. Deviations in gas temperature in the mobility cell as well as

small variations in the position and shape of the nanoESI emitter may lead to random drift in the distributions of di-Ub ions.[36] To compensate for these deviations, we introduced an internal calibrant to calibrate collision cross sections (CCS) across di-Ub isomers. We chose apo-myoglobin because its molecular weight and charge distribution are similar to di-Ub and its signal does not overlap with that of di-Ub in the mobility spectra (**Figure S1**). Moreover, the CCS values of apo-myoglobin added as an internal or external standard only deviate by 0.6% from the reference values (**Table S1**).[37]

The inclusion of a single internal calibrant may cause significant systematic error in CCS values,[38] however, we found that the systematic error is only 1.2% and the random error is lower with apo-myoglobin as an internal versus external calibrants (**Figure S2**). The systematic error could be further reduced using multiple internal calibrants instead, but precise CCS values are not necessary for accurate quantitation. Moreover, multiple internal standards could complicate the quantitation. Thus, we decided to use a single internal calibrant.

Quantitative analysis of di-Ub isomers. With the addition of apo-myoglobin, we sought to apply a linear deconvolution method to measure the amount of each di-Ub in a binary mixture. A few of the di-Ub isomers, e.g., K29 and K48, exhibit bimodal IM distributions, making it difficult to use gaussian fits with different intensities for quantitation.[39] Thus, we chose to use multiple linear regression analysis, which entailed fitting unknown mixtures to a linear combination of spectra corresponding to individual di-Ub isomers using Euclidean metrics.[40] Weights of each component in a binary mixture (w_i , w_j) were obtained, allowing us to calculate relative weights $q_i = w_i/(w_i + w_j)$ or $q_j = w_j/(w_i + w_j)$ (**Scheme 1**).

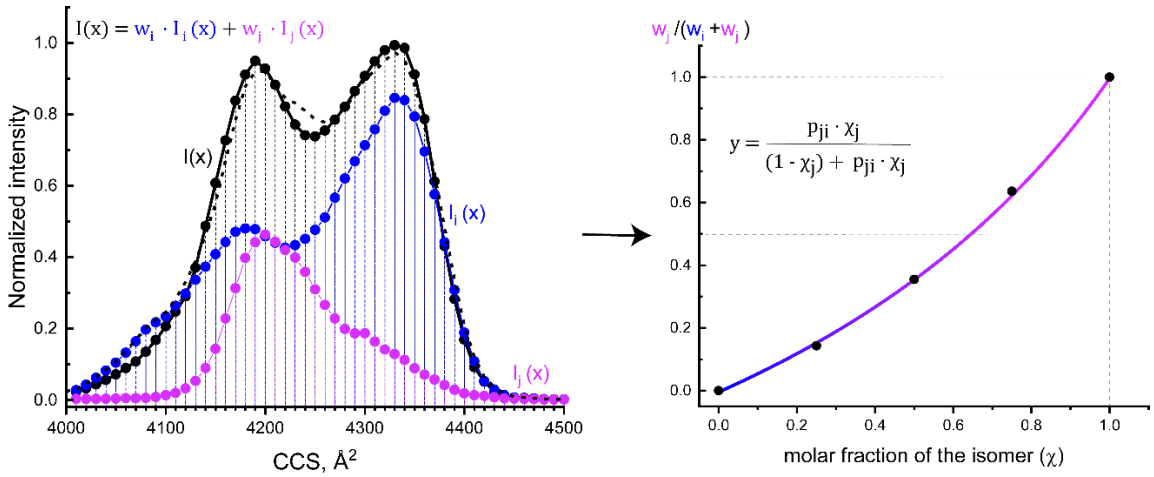

Scheme 1. Spectral deconvolution approach using multiple linear regression analysis. The IM spectrum of a binary mixture (black spectrum) is deconvolved via the IM spectra of single isomers (blue and purple spectra), furnishing the normalized weights of single components that are then be used to create a calibration curve for the calculation of molar fraction of each isomer (χ_i, χ_j; shown on the right) in a mixture. The parameter p_{ji} in the calibration curve relates to ratios of response factors for different isomers (see Eq. 1).

When the IM-MS spectra of individual isomers were used to deconvolute a binary mixture, we observed a non-linear correlation between relative weight and molar fraction (**Figure 2, Figures S3**). Such non-linearity cannot be explained by the deconvolution procedure as the convexity of the calibration curve varies for different pairs of isomers and in some cases is even linear (**Figure S4, S10**). We also found that the non-linear behavior depends on the type of binary mixture analyzed, not the total di-Ub concentration (**Figure S5**). Similar behavior has been previously observed for β-amyloid peptides bearing isomerized aspartic acid residues.[41,42] In this case, the basic version of multiple linear regression analysis was used to determine the relative weights of each isomer in the spectrum. The weights were then adjusted to obtain the actual molar fractions. We thought we could apply similar logic to obtain the molar fractions of individual di-Ub isomers.

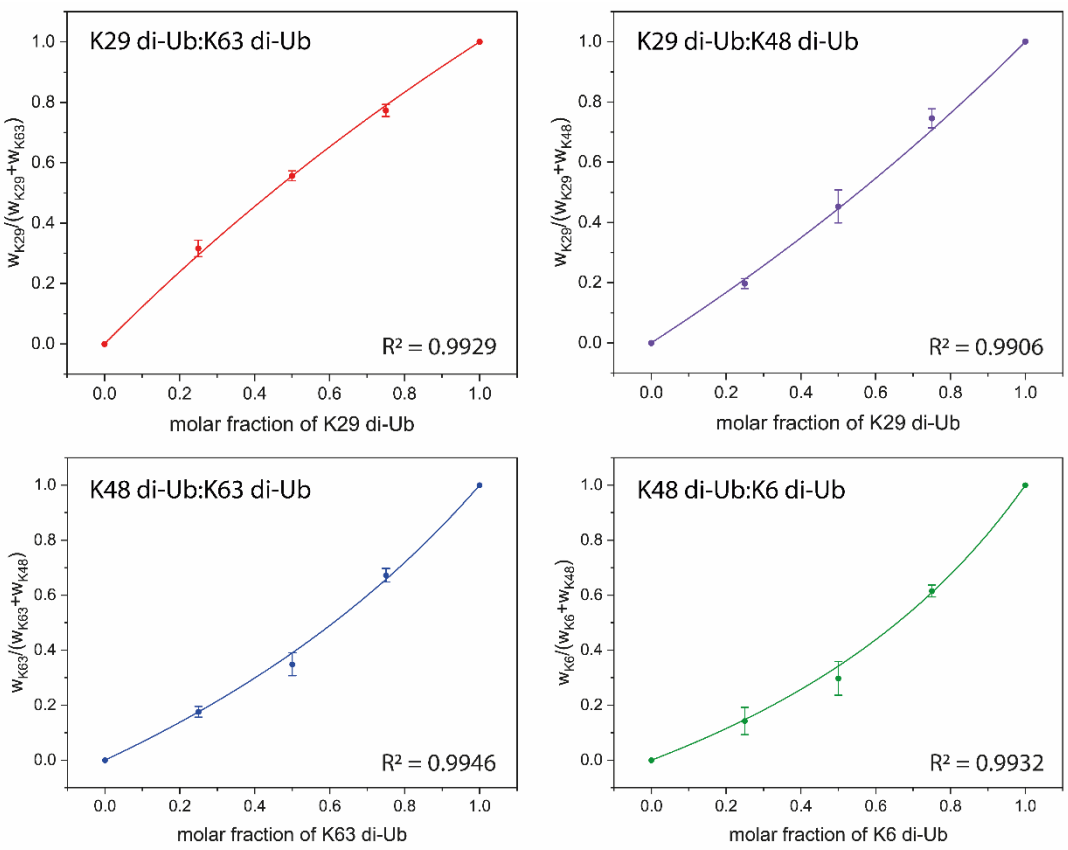

Figure 2. Calibration curves corresponding to different binary mixtures of di-Ub isomers. Fits to Eq. 1 are shown.

Using the 'response factor' k_i, the absolute intensity of a single di-Ub isomer can be related to the total concentration (C) and molar fraction (χ_i) of that isomer. In principle, k_i depends on the (i) overall ion yield in ESI and (ii) the probability that a particular isomer is protonated during ionization. Although the absolute value of k fluctuates with the total ion current of ESI, we can assume that the ratio of k values for different isomers ($p_{ij} = k_i/k_j$ for i and j isomers) remains constant. Based on this assumption, the relative weights ($q_i = w_i/(w_i + w_j)$ and $q_j = w_j/(w_i + w_j)$) of di-Ub isomers "i" and "j" after deconvolution in the IM spectrum should depend on the molar fractions according to (**Equation 1**):

$$q_j = \frac{w_j}{w_j + w_i} = \frac{k_j \chi_j C}{k_i \chi_i C + k_j \chi_j C} = \frac{\frac{k_j}{k_i}\chi_j}{\frac{k_i}{k_i}\chi_i + \frac{k_j}{k_i}\chi_j} = \frac{p_{ji}\chi_j}{\chi_i + p_{ji}\chi_j} = \frac{p_{ji}\chi_j}{(1-\chi_j) + p_{ji}\chi_j} \quad (1)$$

Fitting the deconvoluted spectral data to Eq. 1 led to a good approximation of molar fractions for a variety of binary mixtures (**Figure 2**).

Quantitative approach to multicomponent di-Ub mixtures. Based on the success of deconvoluting di-Ub pairs, we wanted to extend our mathematical model to more complex mixtures. Whether it is a ternary or higher order mixture, the relative weight of a specific isomer (q_i) should depend on the response factor (k) of all isomers (**Equation 2**):

$$q_i = \frac{w_i}{\sum_{j=1}^{n} w_j} = \frac{k_i \chi_i C}{\sum_{j=1}^{n} k_j \chi_j C} = \frac{\frac{k_i}{k_0} \cdot \chi_i}{\sum_{j=1}^{n} \frac{k_j}{k_0} \chi_j} = \frac{p_{i0}\, \chi_i}{\sum_{j=1}^{n} p_{j0}\, \chi_j} \quad (2)$$

Similar to the binary mixtures, it is possible to relate the response factor of one isomer k_i to a 'reference' isomer k_0: $\mathrm{p_{i0}} = \mathrm{k_i}/\mathrm{k_0}$. The reference isomer can be any one of the isomers in the mixture. To obtain the relative response factor values we need to construct the calibration curves for binary mixtures, containing one of the presented isomers "i" and the selected reference isomer "0". The IM spectra for the binary mixtures and the multicomponent mixture should be measured in a single set of experiments. Thus, for multicomponent mixtures the relative response factors p_{i0} cannot be derived from the curves shown in Figure 2 unless the binary calibration curve is generated at the same time with the same external conditions. Once the relative response factor p_{i0} is obtained, the molar fraction can be calculated. This can be achieved by rewriting Eq. 2 as Eq. 3 since $\sum_{i=1}^{n} \chi_i = 1$ (derivation of Eq. 3 is shown in Supporting Information, S17).

$$\chi_i = \frac{q_i / p_{i0}}{\sum_{j=1}^{n} \frac{q_j}{p_{j0}}} \quad (3)$$

Application of quantitative IM-MS to multicomponent di-Ub mixtures.
To deconvolute more complex spectra, we initially applied a full spectral library containing all seven di-Ub isomers. The deconvolution results demonstrate the high specificity of the proposed multiple linear regression analysis. Even in the case of weakly resolved isomers, such as K6- and K11-, the deconvolution procedure successfully identifies the isomers present in the mixture on a qualitative level

(**Figure S6-S7**). These results suggest that for multicomponent mixtures, deconvolution using an entire spectral library is possible; however, for the purposes of quantitation, using the full spectral library can be challenging due to the necessity of calibration curves. As shown in Figure 2, at least five points are necessary to generate a calibration curve, with two points corresponding to pure di-Ub isomers and three representing binary mixtures with different ratios of single components. Hence, the number of samples needed to generate calibration curves for a full spectral library is $(3 \cdot (n-1) + n) \cdot m$, where n is a number of isomers in the library, and m is a number of biological replicates. Since calibration curves and unknown samples must be measured at the same time for accurate quantitation, the concern is that long experimental times may cause significant fluctuations in relative response factors.

To compensate for these issues, we decided to apply a 'reduced' spectral library to quantify molar fractions. Although the reduced library contains only the di-Ub isomers present in a mixture, significantly less experimental time is needed relative to the full library, resulting in little variation in relative response factors. We illustrate the use of a reduced library in the analysis of ternary and quaternary mixtures.

For a ternary mixture containing K6, K29, and K63 isomers, the spectra of pure K6, K29, and K63 di-Ub were used for deconvolution to obtain weights w_{K6}, w_{K29}, and w_{K63} (**Figure 3C**). Using these values, we then calculated relative weights (q_i): $q_{K6}=w_{K6}/(w_{K6}+w_{K29}+w_{K63})$, $q_{K29}= w_{K29}/(w_{K6}+w_{K29}+w_{K63})$, $q_{K63}= w_{K63}/(w_{K6}+w_{K29}+w_{K63})$. In parallel, data was collected to generate calibration curves corresponding to K6/K63 and K29/K63 binary mixtures (**Figure 3A-3B**). With K63 as the reference isomer, we obtained the relative response factors $p_{K6/K63}$ and $p_{K29/K63}$. Combining the p_i and q_i values, we are able to arrive at the molar fraction of each component (**Figure 3E, Equation 3**).

Quaternary mixtures can also be deconvoluted. In this case, the spectral library containing the four isomers K6, K29, K48, and K63, was used to calculate relative weights (q_i) (**Figure 3D**). One additional binary mixture, K48/K63, was measured to obtain all of the necessary relative response factors, including the value for $p_{K48/K63}$

(**Figure 3F, Figure S8**). IM-MS data for approximately thirty ternary and quaternary mixtures were collected to measure the error relative to the actual molar fraction (**Table S2**). A measured error of ≤ 5.2% and a single residue error of 4.8% (SRE corresponds to the difference between the actual and experimental molar fractions for a single type of the isomer) strongly suggests that multiple linear regression analysis can be used to quantify linkage types in mixture of di-Ub isomers (**Figure 3G, Supporting Information S17**).

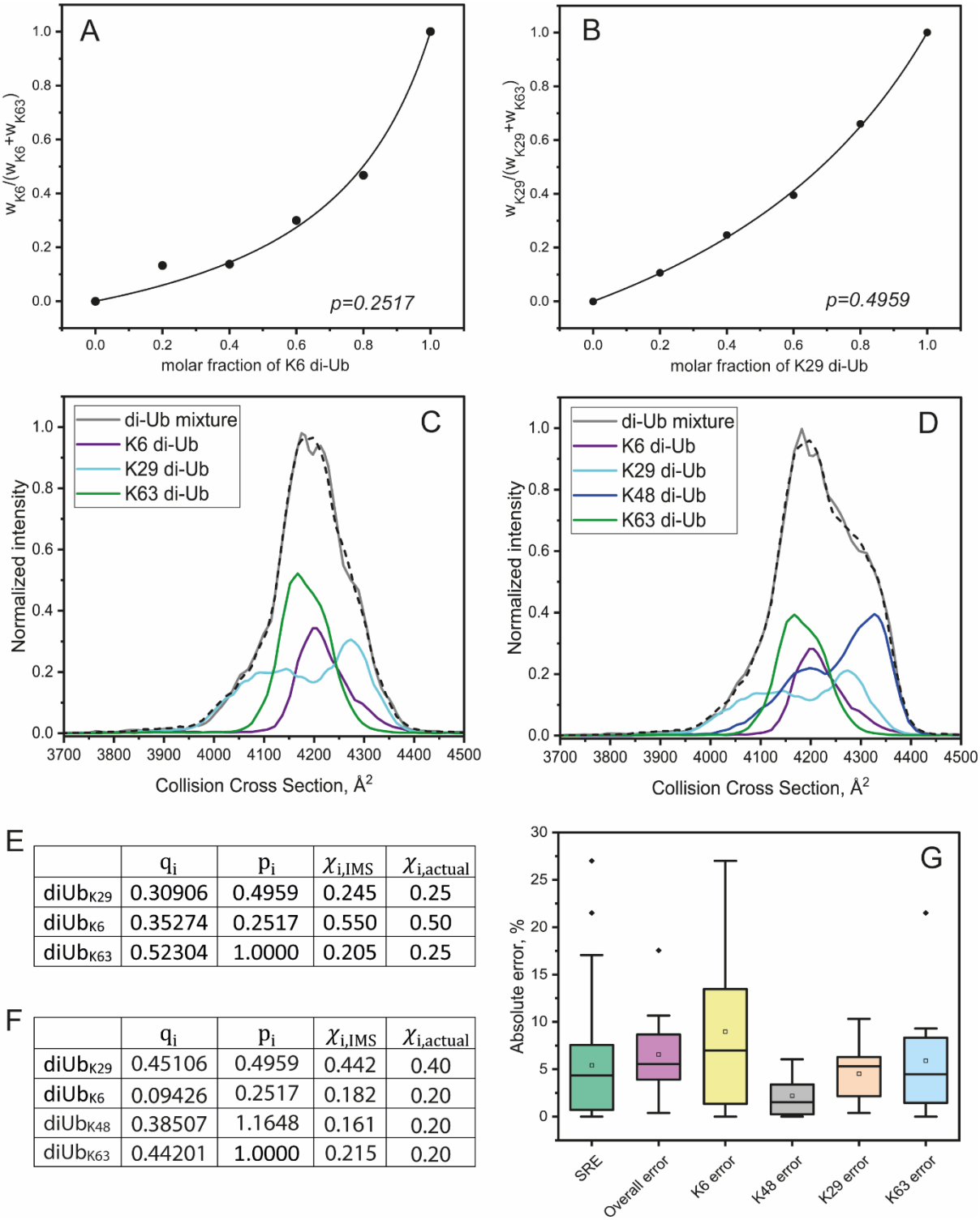

	q_i	p_i	$\chi_{i,IMS}$	$\chi_{i,actual}$
$diUb_{K29}$	0.30906	0.4959	0.245	0.25
$diUb_{K6}$	0.35274	0.2517	0.550	0.50
$diUb_{K63}$	0.52304	1.0000	0.205	0.25

	q_i	p_i	$\chi_{i,IMS}$	$\chi_{i,actual}$
$diUb_{K29}$	0.45106	0.4959	0.442	0.40
$diUb_{K6}$	0.09426	0.2517	0.182	0.20
$diUb_{K48}$	0.38507	1.1648	0.161	0.20
$diUb_{K63}$	0.44201	1.0000	0.215	0.20

Figure 3. Relative quantitation of di-Ub isomers in ternary and quaternary mixtures. Quantitation of each isomer was performed using calibration curves corresponding to binary mixtures. **A-B.** The calibration curves for the ternary mixture are shown. **A.** Calibration curve corresponding to the K6- and K63-linked di-Ub pair. **B.** Calibration curve corresponding to the K29- and K63-linked di-Ub pair. K63 di-Ub was chosen as the reference isomer. **C.** Decomposition of the ternary mixture into spectra

corresponding to pure di-Ub isomers. **D.** Decomposition of the quaternary mixture into spectra corresponding to pure di-Ub isomers. The solid black line corresponds to the actual spectra of the ternary mixture and the dash gray line is a linear fit of the spectrum of a mixture with spectra of single isomers. **E-F**. Relative weights (q_i) and relative response factors (p_{i0}) for each component were used to calculate the molar fraction in ternary and quaternary mixtures. **G.** Statistics of quantitation accuracy for the presented method.

Validation of the IM-based quantitation approach by AQUA analysis. Lastly, we characterized the di-Ub isomers produced by an E3 ligase using our quantitative IM-MS approach. In the presence of the E2 conjugating enzyme UbcH7, the bacterial effector protein NleL, which is an E3 ligase, generates Ub chains primarily composed of K6 and K48 linkages. After purifying the di-Ub fraction of the enzymatic reaction, bottom-up proteomics with isotopically labeled, Ub-derived peptides—a method referred to as AQUA analysis—confirmed the formation and abundance of K6- and K48-linked di-Ub. We then collected the IM-MS spectrum of the di-Ub fraction in the presence of the apo-myoglobin standard and applied multiple linear regression analysis to different charge states. On average, we found that K6-linked di-Ub comprises 75% while K48-linked di-Ub is only 25% of the di-Ub fraction. These data agree with the AQUA analysis (**Figure 4**), demonstrating the robustness of our quantitative IM-MS-based approach.

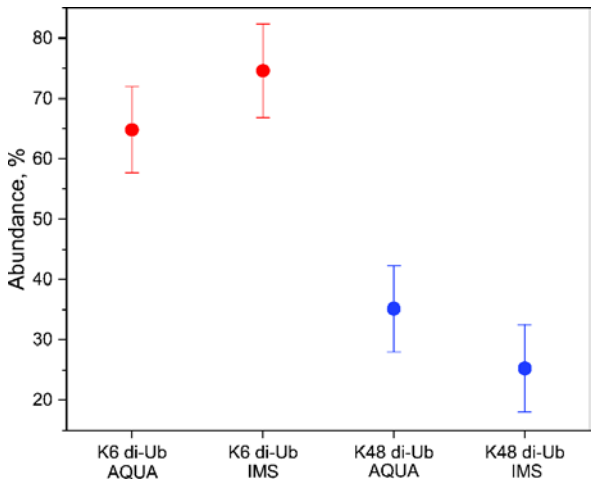

Figure 4. Comparison between AQUA and IM-MS analysis of the enzymatic reaction using the E3 ligase NleL.

CONCLUSIONS

In this work, we develop a mathematical framework for quantifying the relative abundance of di-Ub isomers in complex mixtures using IM-MS. We found that despite the structural similarity, different di-Ub isomers could have significantly different response factors that do not allow linear approximation to convert IM intensities into molar fractions of a particular isomer. Using an internal standard and applying multiple linear regression analysis to the spectral data enables robust quantitation of di-Ub molar fractions in complex mixtures containing up to four different isomers. Our mathematical model can also be used to characterize the types of di-Ub isomers produced by enzymatic reactions. Future efforts will focus on using these methods to characterize mixtures of higher molecular weight Ub conjugates with greater morphological complexity.

ACKNOWLEDGEMENTS

This work was supported by research grant RO1GM110543 from the National Institutes of Health (NIH). The data described herein were acquired on a Waters Synapt G2 HDMS funded by Massachusetts Life Sciences Center and Orbitrap Fusion mass spectrometer funded by National Institutes of Health grant 1S10OD010645-01A1.

REFERENCES

(1) Oh, E.; Akopian, D.; Rape, M. Principles of Ubiquitin-Dependent Signaling. *Annu. Rev. Cell Dev. Biol.* **2018**, *34* (1), 137–162. https://doi.org/10.1146/annurev-cellbio-100617-062802.

(2) Haglund, K.; Dikic, I. Ubiquitylation and Cell Signaling. *EMBO J.* **2005**, *24* (19), 3353–3359. https://doi.org/10.1038/sj.emboj.7600808.

(3) Ciechanover, A.; Schwartz, A. L. The Ubiquitin-Proteasome Pathway: The Complexity and Myriad Functions of Proteins Death. *Proc. Natl. Acad. Sci.* **1998**, *95* (6), 2727–2730. https://doi.org/10.1073/pnas.95.6.2727.

(4) Yao, T.; Ndoja, A. Regulation of Gene Expression by the Ubiquitin-Proteasome System. *Semin. Cell Dev. Biol.* **2012**, *23* (5), 523–529. https://doi.org/10.1016/j.semcdb.2012.02.006.

(5) Vucic, D.; Dixit, V. M.; Wertz, I. E. Ubiquitylation in Apoptosis: A Post-Translational Modification at the Edge of Life and Death. *Nat. Rev. Mol. Cell Biol.* **2011**, *12* (7), 439–452. https://doi.org/10.1038/nrm3143.

(6) Nath, D.; Shadan, S. The Ubiquitin System. *Nature* **2009**, *458* (7237), 421–421. https://doi.org/10.1038/458421a.

(7) Deol, K. K.; Lorenz, S.; Strieter, E. R. Enzymatic Logic of Ubiquitin Chain Assembly. *Front. Physiol.* **2019**, *10* (July), 1–14. https://doi.org/10.3389/fphys.2019.00835.

(8) Komander, D.; Rape, M. The Ubiquitin Code. *Annu. Rev. Biochem.* **2012**, *81* (1), 203–229. https://doi.org/10.1146/annurev-biochem-060310-170328.

(9) Ohtake, F.; Tsuchiya, H. The Emerging Complexity of Ubiquitin Architecture. *J. Biochem.* **2016**, *161* (2), mvw088. https://doi.org/10.1093/jb/mvw088.

(10) Akutsu, M.; Dikic, I.; Bremm, A. Ubiquitin Chain Diversity at a Glance. *J. Cell Sci.* **2016**, *129* (5), 875–880. https://doi.org/10.1242/jcs.183954.

(11) French, M. E.; Koehler, C. F.; Hunter, T. Emerging Functions of Branched Ubiquitin Chains. *Cell Discov.* **2021**, *7* (1), 6. https://doi.org/10.1038/s41421-020-00237-y.

(12) Tracz, M.; Bialek, W. Beyond K48 and K63: Non-Canonical Protein Ubiquitination. *Cell. Mol. Biol. Lett.* **2021**, *26* (1), 1. https://doi.org/10.1186/s11658-020-00245-6.

(13) Harper, J. W.; Bennett, E. J. Proteome Complexity and the Forces That Drive Proteome Imbalance. *Nature* **2016**, *537* (7620), 328–338.

https://doi.org/10.1038/nature19947.

(14) Gao, Y.; Yates, J. R. Protein Analysis by Shotgun Proteomics. In *Mass Spectrometry-Based Chemical Proteomics*; Wiley, 2019; pp 1–38. https://doi.org/10.1002/9781118970195.ch1.

(15) Gundry, R. L.; White, M. Y.; Murray, C. I.; Kane, L. A.; Fu, Q.; Stanley, B. A.; Van Eyk, J. E. Preparation of Proteins and Peptides for Mass Spectrometry Analysis in a Bottom-Up Proteomics Workflow. In *Current Protocols in Molecular Biology*; John Wiley & Sons, Inc.: Hoboken, NJ, USA, 2009; pp 1–23. https://doi.org/10.1002/0471142727.mb1025s88.

(16) Geis-Asteggiante, L.; Lee, A. E.; Fenselau, C. Analysis of the Topology of Ubiquitin Chains. In *Methods in Enzymology*; Elsevier Inc., 2019; Vol. 626, pp 323–346. https://doi.org/10.1016/bs.mie.2019.06.025.

(17) Peng, J.; Schwartz, D.; Elias, J. E.; Thoreen, C. C.; Cheng, D.; Marsischky, G.; Roelofs, J.; Finley, D.; Gygi, S. P. A Proteomics Approach to Understanding Protein Ubiquitination. *Nat. Biotechnol.* **2003**, *21* (8), 921–926. https://doi.org/10.1038/nbt849.

(18) Xu, G.; Paige, J. S.; Jaffrey, S. R. Global Analysis of Lysine Ubiquitination by Ubiquitin Remnant Immunoaffinity Profiling. *Nat. Biotechnol.* **2010**, *28* (8), 868–873. https://doi.org/10.1038/nbt.1654.

(19) Kim, W.; Bennett, E. J.; Huttlin, E. L.; Guo, A.; Li, J.; Possemato, A.; Sowa, M. E.; Rad, R.; Rush, J.; Comb, M. J.; Harper, J. W.; Gygi, S. P. Systematic and Quantitative Assessment of the Ubiquitin-Modified Proteome. *Mol. Cell* **2011**, *44* (2), 325–340. https://doi.org/10.1016/j.molcel.2011.08.025.

(20) Ordureau, A.; Münch, C.; Harper, J. W. Quantifying Ubiquitin Signaling. *Mol. Cell* **2015**, *58* (4), 660–676. https://doi.org/10.1016/j.molcel.2015.02.020.

(21) Phu, L.; Izrael-Tomasevic, A.; Matsumoto, M. L.; Bustos, D.; Dynek, J. N.; Fedorova, A. V.; Bakalarski, C. E.; Arnott, D.; Deshayes, K.; Dixit, V. M.; Kelley, R. F.; Vucic, D.; Kirkpatrick, D. S. Improved Quantitative Mass Spectrometry Methods for Characterizing Complex Ubiquitin Signals. *Mol. Cell. Proteomics* **2011**, *10* (5), M110.003756. https://doi.org/10.1074/mcp.M110.003756.

(22) Kirkpatrick, D. S.; Hathaway, N. A.; Hanna, J.; Elsasser, S.; Rush, J.; Finley, D.; King, R. W.; Gygi, S. P. Quantitative Analysis of in Vitro Ubiquitinated Cyclin B1 Reveals Complex Chain Topology. *Nat. Cell Biol.* **2006**, *8* (7), 700–

710. https://doi.org/10.1038/ncb1436.

(23) Deol, K. K.; Strieter, E. R. The Ubiquitin Proteoform Problem. *Curr. Opin. Chem. Biol.* **2021**, *63*, 95–104. https://doi.org/10.1016/j.cbpa.2021.02.015.

(24) Cannon, J. R.; Martinez-Fonts, K.; Robotham, S. A.; Matouschek, A.; Brodbelt, J. S. Top-Down 193-Nm Ultraviolet Photodissociation Mass Spectrometry for Simultaneous Determination of Polyubiquitin Chain Length and Topology. *Anal. Chem.* **2015**, *87* (3), 1812–1820. https://doi.org/10.1021/ac5038363.

(25) Rana, A. S. J. B.; Ge, Y.; Strieter, E. R. Ubiquitin Chain Enrichment Middle-Down Mass Spectrometry (UbiChEM-MS) Reveals Cell-Cycle Dependent Formation of Lys11/Lys48 Branched Ubiquitin Chains. *J. Proteome Res.* **2017**, *16* (9), 3363–3369. https://doi.org/10.1021/acs.jproteome.7b00381.

(26) Crowe, S. O.; Rana, A. S. J. B.; Deol, K. K.; Ge, Y.; Strieter, E. R. Ubiquitin Chain Enrichment Middle-Down Mass Spectrometry Enables Characterization of Branched Ubiquitin Chains in Cellulo. *Anal. Chem.* **2017**, *89* (8), 4428–4434. https://doi.org/10.1021/acs.analchem.6b03675.

(27) Swatek, K. N.; Usher, J. L.; Kueck, A. F.; Gladkova, C.; Mevissen, T. E. T.; Pruneda, J. N.; Skern, T.; Komander, D. Insights into Ubiquitin Chain Architecture Using Ub-Clipping. *Nature* **2019**, *572* (7770), 533–537. https://doi.org/10.1038/s41586-019-1482-y.

(28) Gabelica, V.; Marklund, E. Fundamentals of Ion Mobility Spectrometry. *Curr. Opin. Chem. Biol.* **2018**, *42*, 51–59. https://doi.org/10.1016/j.cbpa.2017.10.022.

(29) Lanucara, F.; Holman, S. W.; Gray, C. J.; Eyers, C. E. The Power of Ion Mobility-Mass Spectrometry for Structural Characterization and the Study of Conformational Dynamics. *Nat. Chem.* **2014**, *6* (4), 281–294. https://doi.org/10.1038/nchem.1889.

(30) Zhong, Y.; Han, L.; Ruotolo, B. T. Collisional and Coulombic Unfolding of Gas-Phase Proteins: High Correlation to Their Domain Structures in Solution. *Angew. Chemie Int. Ed.* **2014**, *53* (35), 9209–9212. https://doi.org/10.1002/anie.201403784.

(31) Laszlo, K. J.; Bush, M. F. Effects of Charge State, Charge Distribution, and Structure on the Ion Mobility of Protein Ions in Helium Gas: Results from Trajectory Method Calculations. *J. Phys. Chem. A* **2017**, *121* (40), 7768–7777. https://doi.org/10.1021/acs.jpca.7b08154.

(32) Wagner, N. D.; Russell, D. H. Defining Noncovalent Ubiquitin Homodimer

Interfacial Interactions through Comparisons with Covalently Linked Diubiquitin. *J. Am. Chem. Soc.* **2016**, *138* (51), 16588–16591. https://doi.org/10.1021/jacs.6b09829.

(33) Jung, J. E.; Pierson, N. A.; Marquardt, A.; Scheffner, M.; Przybylski, M.; Clemmer, D. E. Differentiation of Compact and Extended Conformations of Di-Ubiquitin Conjugates with Lysine-Specific Isopeptide Linkages by Ion Mobility-Mass Spectrometry. *J. Am. Soc. Mass Spectrom.* **2011**, *22* (8), 1463–1471. https://doi.org/10.1007/s13361-011-0158-0.

(34) Wagner, N. D.; Clemmer, D. E.; Russell, D. H. ESI-IM-MS and Collision-Induced Unfolding That Provide Insight into the Linkage-Dependent Interfacial Interactions of Covalently Linked Diubiquitin. *Anal. Chem.* **2017**, *89* (18), 10094–10103. https://doi.org/10.1021/acs.analchem.7b02932.

(35) Haynes, S. E.; Polasky, D. A.; Dixit, S. M.; Majmudar, J. D.; Neeson, K.; Ruotolo, B. T.; Martin, B. R. Variable-Velocity Traveling-Wave Ion Mobility Separation Enhancing Peak Capacity for Data-Independent Acquisition Proteomics. *Anal. Chem.* **2017**, *89* (11), 5669–5672. https://doi.org/10.1021/acs.analchem.7b00112.

(36) Sun, Y.; Vahidi, S.; Sowole, M. A.; Konermann, L. Protein Structural Studies by Traveling Wave Ion Mobility Spectrometry: A Critical Look at Electrospray Sources and Calibration Issues. *J. Am. Soc. Mass Spectrom.* **2016**, *27* (1), 31–40. https://doi.org/10.1007/s13361-015-1244-5.

(37) Bush, M. F.; Hall, Z.; Giles, K.; Hoyes, J.; Robinson, C. V.; Ruotolo, B. T. Collision Cross Sections of Proteins and Their Complexes: A Calibration Framework and Database for Gas-Phase Structural Biology. *Anal. Chem.* **2010**, *82* (22), 9557–9565. https://doi.org/10.1021/ac1022953.

(38) Ruotolo, B. T.; Benesch, J. L. P.; Sandercock, A. M.; Hyung, S.-J.; Robinson, C. V. Ion Mobility–Mass Spectrometry Analysis of Large Protein Complexes. *Nat. Protoc.* **2008**, *3* (7), 1139–1152. https://doi.org/10.1038/nprot.2008.78.

(39) Polasky, D. A.; Dixit, S. M.; Fantin, S. M.; Ruotolo, B. T. CIUSuite 2: Next-Generation Software for the Analysis of Gas-Phase Protein Unfolding Data. *Anal. Chem.* **2019**, *91* (4), 3147–3155. https://doi.org/10.1021/acs.analchem.8b05762.

(40) Hogan, M. A.; Yamamoto, S.; Covell, D. F. Multiple Linear Regression Analysis of Scintillation Gamma-Ray Spectra: Automatic Candidate Selection. *Nucl.*

Instruments Methods **1970**, *80* (1), 61–68. https://doi.org/10.1016/0029-554X(70)90298-3.

(41) Ivanov, D. G.; Indeykina, M. I.; Pekov, S. I.; Iusupov, A. E.; Bugrova, A. E.; Kononikhin, A. S.; Nikolaev, E. N.; Popov, I. A. Probabilistic Model Applied to Ion Abundances in Product-Ion Spectra: Quantitative Analysis of Aspartic Acid Isomerization in Peptides. *Anal. Bioanal. Chem.* **2019**, *411* (29), 7783–7789. https://doi.org/10.1007/s00216-019-02174-6.

(42) Ivanov, D. G.; Indeykina, M. I.; Pekov, S. I.; Bugrova, A. E.; Kechko, O. I.; Iusupov, A. E.; Kononikhin, A. S.; Makarov, A. A.; Nikolaev, E. N.; Popov, I. A. Relative Quantitation of Beta-Amyloid Peptide Isomers with Simultaneous Isomerization of Multiple Aspartic Acid Residues by Matrix Assisted Laser Desorption Ionization-Time of Flight Mass Spectrometry. *J. Am. Soc. Mass Spectrom.* **2020**, *31* (1), 164–168. https://doi.org/10.1021/jasms.9b00025.